Investigation of oxygen vacancies in CeO_2/Pt system with synchrotron light techniques

2016 J. Phys.: Conf. Ser. 712 012064

(http://iopscience.iop.org/1742-6596/712/1/012064)

Investigation of oxygen vacancies in CeO_2/Pt system with synchrotron light techniques

L Braglia[1,2], A L Bugaev[2], K A Lomachenko[1,2], A V Soldatov[2], C Lamberti[1,2], A A Guda[2]

[1] Department of Chemistry, NIS and CrisDi Centers, Turin University and INSTM Reference Center, 10125 Turin, Italy
[2] International Research Center "Smart Materials", Southern Federal University, 344090 Rostov-on-Don, Russia

luca.braglia@unito.it

Abstract. A peculiar property of ceria is the ease to form oxygen vacancies, producing reactive sites or facilitating ionic diffusion. For these reasons ceria promotes catalytic activities for a number of important reactions when it is used as a support for transition metals. In our work we study the temporal evolution of oxygen vacancies formation by time-resolved XANES at Ce K-edge and XRD measurements on CeO_2/Pt nanoparticles, successfully monitoring the reaction of CO oxidation.

1. Introduction

This rare earth oxide claim several applications: in catalysis as a support substrate to improve mechanical and thermal stability and moreover as activity and selectivity of catalysis. Ceria also covers an important role in treatment of toxic emissions, for removal soot from diesel engine exhaust, as integral part of car exhaust three-way automotive catalysts, in low-temperature water-gas shift reaction, in solid oxide fuel lattices (SOFCs), in solar-driven thermochemical CO_2 reduction and for biomass reforming [1]. The reason of these wide range of applications is enclosed in the high oxygen storage capacity (OSC) at low temperature, which is the capacity to store oxygen at lean and to release it at rich condition. We focused our attention in the CO oxidation process [2]: $2Ce^{4+}+O^{2-}+CO \rightarrow 2Ce^{3+}+V_o+CO_2$, where O^{2-} is lattice oxygen and V_o is oxygen vacancy. The CO molecules are absorbed on the surface of Pt nanoparticles, where they react with the oxygen provided by non-stoichiometric cerium oxide [3]. Hence, Ce^{3+} concentration, which can be monitored by x-ray absorption spectroscopy [4], is proportionally related with oxygen vacancy concentration. The presence of noble and transition metals facilitate the release of oxygen from ceria, and they actively participate to the catalysis process [5]. However the kinetics of this process that is determined by energy of activation is still unclear. DFT studies predict that energy, required for oxygen atom to migrate from one crystallographic position into another depends on concentration of vacancies and is in the range of 0.46–1.08 eV [6]. *Hui-Ying Li et al.* [7] found out that the most energy favourable mechanism of oxygen vacancy on the surface of CeO_2 in 111 plane is the two-step (TS) diffusion [8]. In this work we analyse the process of vacancy formation by means of monitoring Ce^{3+} concentration.

2. Experimental and Methods

The change in the oxidation state of Ce^{4+} in Ce^{3+} during the reaction with CO, previously described, permitted the monitoring of the temporal evolution of Ce^{3+} formation with a suitable technique as time-resolved X-ray absorption near-edge spectroscopy (XANES). During the Ce reduction we also observed a change of lattice parameter that it has been studied with powder X-ray diffraction (XRD).
Truncated octahedral CeO_2 nanoparticles were prepared by hydrothermal method. The platinum nanoparticles were deposited on ceria by wetness impregnation by tetraammine platinum(II) nitrate (Aldrich, 99.995%) followed by calcination in air at 674K for 4 h and reduction in 5% H_2 flow at 573K for 4 h [2]. The diameter of platinum nanoparticles is 1.2 (±0.2) nm, and the concentration is 1.5%wt.
We collected the XANES spectra at BM23 beamline of ESRF (Grenoble, France) at Ce K-edge (40470eV). The measurement has been done in transmission mode using a double-crystal monochromator Si (311). Powder sample was introduced within a glass capillary of 1 mm diameter size and the gas was capable to flow through the two cut edges of the capillary. We measured the steady XANES spectra at 473K in O_2, afterwards we switched in reducing flow of CO, following the temporal evolution of Ce^{3+} formation collecting the XANES spectra for 3 h 15 min. The same procedure has been adopted for collecting the two-dimensional XRD patterns (λ=0.3024 Å) at BM23 beamline. The data were analyzed with Athena software and then the principal component analysis (PCA) [9] has been done with FitIt software [10].

3. Results and Discussion

XAS has proved an attractive technique for monitoring the temporal evolution of the Ce^{3+} formation in reductive condition. In figure 1a are reported the Ce K-edge XANES spectra of the sample at the steady state in O_2 (blue curve) and in CO (orange curve) after 3 h 15 min of reaction. The changes are slightly small but visible: in CO the absorption threshold of the XANES spectrum is shifted to lower energy and the shape of the second peak is shifted to lower energy indicating increase of Ce-O distances. The energy shift of the absorption threshold confirms the reduction of Ce^{4+} in Ce^{3+} in CO flux.

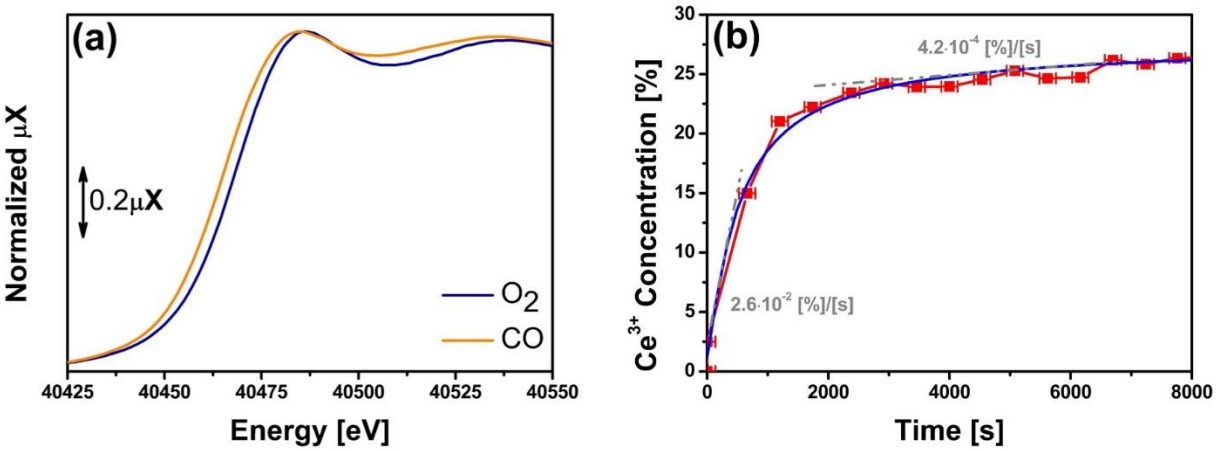

Figure 1. (a) XANES spectra at 423K above Ce K-edge of the CeO_2/Pt nanoparticles in the steady state in O_2 (blue line) and in presence of CO (orange line) after 3 h 15 min of reaction; (b) Temporal evolution of Ce^{3+} formation in reductive condition in function of time at 423K. PCA analysis was performed on the XANES spectra collected at Ce K-edge in CO. We fitted the curve with an exponential function (blue line) and we have drawn the tangents in grey coloured with their respectively slope values.

Principal component analysis (PCA) was performed for series of XANES spectra during the CO fluxing and revealed two independent components. We associated the components to Ce^{3+} and Ce^{4+} state and in

PCA results we observed an exponential time dependent behaviour of the Ce^{3+} formation, shown in figure 1b. The concentration has been figured out considering as references, the XANES spectra of $Ce_2(CO_3)_3$ for 100% Ce^{3+} and the spectrum of CeO_2/Pt nanoparticles in O_2 for 0% Ce^{3+} ; the XAS measurement was performed in previously experiment [2] and the output of the sample cell was connected to the mass spectrometer allowing to follow the CO_2 formation. The trend of the curve in figure 1b presents a drastic rise until 20% corresponding to the percentage of Ce^{3+} formation in the first 20 min that undergoes to a significant decrease of the rate reaching a plateau at around 25% of Ce^{3+}%. The plot in figure 1b can be divided in two regions: region I, which occurs during the first 20 min of flow in CO, where the CO molecules absorbed on Pt surface react with the oxygen provided by the CeO_2 surface with the following reduction of Ce^{4+} atoms. This mechanism yields an increasing of the oxygen vacancies in the local area around Pt nanoparticles and on the surface of ceria, leading a lack of available O atoms for the reaction with CO absorbed on Pt surface. In region II we observed that the rate of Ce^{3+} formation rapidly decrease, possibly in association with the oxygen migration from the bulk to the surface. We estimated the rate of Ce^{3+}% formation in the two regions mentioned before, drawing the two tangents for the respectively parts. The tangent in the region I, reported in figure 1b, presents a slope of 2.6×10^{-2} [%]/[s], conversely the slope achieved in the region II, where the Ce^{3+}% formation is much slower, is 4.2×10^{-4} [%]/[s]. The value of the rate obtained in the second region provides information about the oxygen vacancy formation that is directly related with the Ce^{3+} formation.
Cerium forms non-stoichiometric oxides with the fluorite structure ($Fm\bar{3}m$). The effect of Ce^{3+} formation can be also supported with the variation of lattice parameter distances, hence we collected powder XRD patterns with the same setup and procedure used previously for XAS experiment. In figure 2a are shown the XRD patterns for the steady state of the sample in O_2 (blue line) and in CO (orange line), and as seen before we collected XRD patterns during the flux of CO in function of time, following the temporal variation of the lattice parameter. The lattice parameter has been derived for each XRD patterns and we distinguished an expansion of the lattice parameter, shown in figure 2b, due to the loss of oxygen atoms, that its behaviour can be described by an exponential curve.

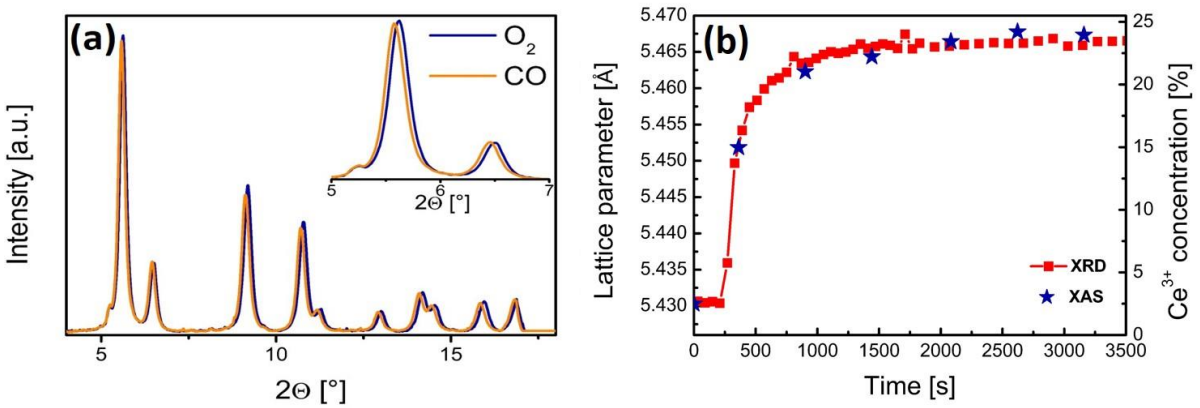

Figure 2. (a) The XRD patterns (λ=0.3024 Å) at 423K are shown in completely oxidized state in O_2 (blue line) and in reduced state in CO (orange line). (b) Lattice parameter variation in time dependent (red line) after the CO switching derived from the XRD patterns. The blue star scatter indicate the values of the temporal evolution of Ce^{3+} formation described by XANES spectra previously seen in figure 1b.

The curve in figure 2b reproduced the trend studied with XAS measurements, indeed in the first 20 min there is an intense rise of the lattice parameter value, correspondingly the high Ce^{3+} formation, which undergoes to a quick slowdown.

4. Conclusions

XANES experiments have proved the formation of Ce^{3+} in the CeO_2/Pt nanoparticles in presence of CO. Collecting series of XANES spectra in CO and with a further PCA analysis we have figured out the exponential behaviour of the Ce^{3+} formation and the Ce^{3+}% concentrations during the reaction. In 3h 15min in CO, the sample formed ≈ 25% of Ce^{3+} atoms in two main steps, described by the exponential fit in figure 1b: in 20 min the Ce^{3+} formation is rapid until 20% and then bear to a significant slowdown of the rate. The rate of Ce^{3+} and oxygen vacancies formation in the region II is slow and can be related with the migration of oxygen atoms from the bulk to the interface with Pt nanoparticles. The combination of XAS and XRD techniques has been very useful because the Ce^{3+} formation is accompanied by an expansion of the lattice parameter that it has been studied in CO and we observed a similar exponential tendency, shown in figure 2b. X-ray Photoelectron Spectroscopy (XPS) performed at the same environmental condition could be an interesting technique to study more in detail the temporal evolution of oxygen migration, varying the kinetic energy of photoelectrons, the probing depth changes and the oxygen vacancy concentration could be monitored at different depth [11].

Acknowledgements

A.B., K.L., A.G. acknowledge the Grant of the President of Russia for Young Scientists MK-3206.2014.2. A.S. and C.L. acknowledge the Mega-grant of the Russian Federation Government to support scientific research under the supervision of the leading scientist at Southern Federal University, No. 14.Y26.31.0001, for the partial funding of the research. L.B. acknowledge Master in Material Science Exploiting Large Scale Facilities (MaMaSELF programme). We also acknowledge O. Safonova from Paul Scherer Institute (PSI, Villigen, Switzerland) who provided the samples.

References

[1] Li S L, Wang N L, Yue Y H, Wang G S, Zu Z, and Zhang Y 2015 *Chem. Sci.* **6** 2495-500
[2] Safonova O V, Guda A A, Paun C, Smolentsev N, Abdala P M, Smolentsev G, Nachtegaal M, Szlachetko J, Soldatov M A, Soldatov A V *et al.* 2014 *J. Phys. Chem. C* **118** 1974-82
[3] Gorte R J 2010 *Aiche J.* **56** 1126-35
[4] Rothensteiner M, Sala S, Bonk A, Vogt U, Emerich H, and van Bokhoven J A 2015 *Phys. Chem. Chem. Phys.* **17** 26988-96
[5] Trovarelli A, Catalysis by ceria and related materials, Imperial College Press, London, 2002.
[6] Vayssilov G N, Lykhach Y, Migani A, Staudt T, Petrova G P, Tsud N, Skala T, Bruix A, Illas F, Prince K C *et al.* 2011 *Nat. Mater.* **10** 310-5
[7] Li H Y, Wang H F, Guo Y L, Lu G Z, and Hu P 2011 *Chem. Commun.* **47** 6105-7
[8] Wang H F, Li H Y, Gong X Q, Guo Y L, Lu G Z, and Hu P 2012 *Phys. Chem. Chem. Phys.* **14** 16521-35
[9] Beale A M, Le M T, Hoste S, and Sankar G 2005 *Solid State Sci.* **7** 1141-8
[10] Smolentsev G and Soldatov A V 2007 *Comput. Mater. Sci.* **39** 569-74
[11] Kato S, Ammann M, Huthwelker T, Paun C, Lampimaki M, Lee M T, Rothensteiner M, and van Bokhoven J A 2015 *Phys. Chem. Chem. Phys.* **17** 5078-83